Available online at www.sciencedirect.com
SCIENCE DIRECT®
Carbohydrate Research 340 (2005) 2212–2217
Carbohydrate RESEARCH

Note

^{1}H and ^{13}C NMR characterization and secondary structure of the K2 polysaccharide of *Klebsiella pneumoniae* strain 52145

Maria Michela Corsaro,[a,*] Cristina De Castro,[a] Teresa Naldi,[a] Michelangelo Parrilli,[a] Juan M. Tomás[b] and Miguel Regué[c]

[a]*Dipartimento di Chimica Organica e Biochimica Università Federico II di Napoli, Complesso Universitario Monte Sant'Angelo Via Cintia 4, 80126 Napoli, Italy*
[b]*Departamento de Microbiología, Universidad de Barcelona, Av Diagonal 645, 08071 Barcelona, Spain*
[c]*Departamento de Microbiología y Parasitología Sanitarias, Universidad de Barcelona, Av Joan XXIII, 08028 Barcelona, Spain*

Received 24 February 2005; received in revised form 11 July 2005; accepted 12 July 2005
Available online 28 July 2005

Abstract—The complete ^{1}H and ^{13}C NMR characterization of the tetrasaccharide repeating unit from the K2 polysaccharide of *Klebsiella pneumoniae* strain 52145 is reported.

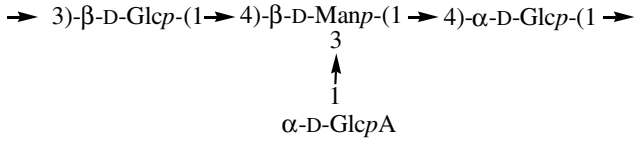

In addition a model for its secondary structure was suggested on the basis of dynamic and molecular calculations.

Keywords: *Klebsiella pneumoniae*; Capsular polysaccharide; NMR spectroscopy; Molecular modelling

Klebsiella pneumoniae, belonging to the family of *Enterobacteriaceae*, is a well known opportunistic nosocomial pathogen responsible for several infections, which usually involve the urinary and the respiratory tracts in immunocompromised individuals. This genus generally develops prominent capsules, which form thick bundles of fibrillose structures covering the bacterial surface in the bulky layer. In addition to protect the bacterium from phagocytosis by granulocytes and bactericidal serum factors these capsules are considered essential to the virulence of the bacterium. From a chemical point of view, the capsules are complex acidic polysaccharides (CPS) consisting of repeating units composed of four to six sugars, one of which is often an uronic acid. These capsules can be classified into 77 serological K antigen types, whose virulence degree seems to be correlated with the type of monosaccharide present in the repeating unit. If the monosaccharide is recognized by a surface lectin of macrophages the bacterium is phagocytosed. The absence of repetitive sequence of D-mannose-α-2,3-D-mannose or L-rhamnose-α-2,3-L-rhamnose in the capsular polysaccharides seems to imply a high virulence, as in the case of K2 strains, which are the most commonly found in *Klebsiella* isolated from infected individuals.[1] Notwithstanding the importance of the K2 serotype strains the structure of the K2 antigen is based only on chemical and/or phage-induce degradative analyses with a poor nuclear magnetic resonance characterization.

This letter describes the complete ^{1}H and ^{13}C NMR characterization of the tetrasaccharide repeating unit

* Corresponding author. Tel.: +39 081674149; fax: +39 081674393; e-mail: corsaro@unina.it

0008-6215/$ - see front matter © 2005 Elsevier Ltd. All rights reserved.
doi:10.1016/j.carres.2005.07.006

from the K2 polysaccharide of *K. pneumoniae* strain 52145. The structure was described for the first time by Gahan et al.[2] for *Aerobacter aerogens* and it is reported here

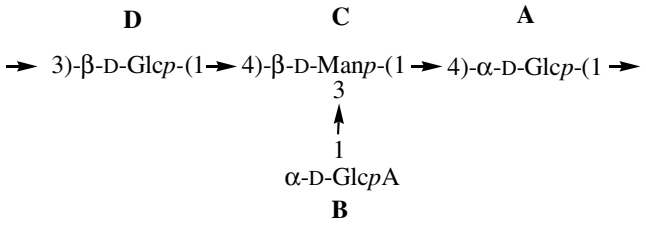

Their structural determination was based on the chemical degradative methods and the ^{1}H NMR analysis was only limited to the determination of the linkage configuration on the basis of the chemical shift values of the degraded oligosaccharides anomeric protons. Sutherland[3] found the same structure from different *Klebsiella* type 2 strains by enzymatic degradation but no NMR analysis was reported.

K. pneumoniae strain 52145 is characterized by two main surface antigens, the O1-LPS and the K2 capsule.[4] The capsular polysaccharide (CPS) was isolated from the aqueous phase of the phenol/water extract of *K. pneumoniae* strain 52145 containing mutations in the *wabH* and *waaL* genes. This mutant was chosen because the double mutation results in a truncated core LPS devoid of O-antigen, thus facilitating its capsule isolation, purification and analysis. In order to eliminate nucleic acids and lipopolysaccharides this sample was submitted to hydrophobic chromatography on a Butyl Sepharose column (Pharmacia), obtaining three main fractions, named **1**, **2** and **3**, respectively. Fraction **2** contained only nucleic acids, while in fraction **1** and **3** the LPS and the CPS were co-eluted, as reported by Izquierdo et al.[5] Only fraction **1** was used for isolation of LPS free CPS, as it contained the higher amount of CPS. Fraction **1** was hydrolyzed with 1% AcOH in order to remove the lipid A moiety. After precipitation and centrifugation, the supernatant liquid was chromatographed on a Sephacryl S 300 column (Pharmacia) to give the pure CPS.

The glycosyl composition, obtained by analysis of acetylated methyl glycosides, indicated a monosaccharide composition consisting of glucose, mannose and glucuronic acid. The absolute configuration of these sugars was determined to be D on the basis of the GLC–MS analysis of their 2-octyl glycoside acetates.[6] The results of the methylation analysis showed the presence of 3,4-linked mannose units, 4-linked glucose units, 3-linked glucose units and terminal glucuronic acid units.

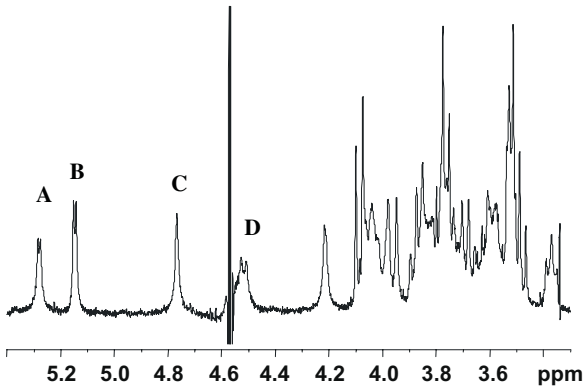

Figure 1. ^{1}H NMR of *K. pneumoniae* K2 polysaccharide in D_2O at 313 K and pD = 7.

The ^{1}H NMR spectrum (Fig. 1) measured in D_2O at pD = 7 and 313 K showed four anomeric signals of similar intensity occurring at δ 5.283 (d, $^3J_{H\text{-}1,H\text{-}2} = 3.7$ Hz), 5.152 (d, $^3J_{H\text{-}1,H\text{-}2} = 3.5$ Hz), 4.769 (br s) and 4.518 (d, $^3J_{H\text{-}1,H\text{-}2} = 7.0$ Hz) indicating a regular tetrasaccharide (**A**–**D**, in decreasing chemical shift order) repeating unit. Both chemical shift and vicinal coupling constant values were in a good agreement with an α anomeric configuration for the first two residues and a β one for the fourth. The signal at 4.769 ppm was assigned to the β-mannopyranose unit on the basis of its broad singlet appearance and its rather high field chemical shift. Starting from these anomeric signals the complete scalar connectivity of the residues **A**, **B** and **D** was assigned both by COSY and TOCSY 2D NMR experiments (Table 1), allowing the identification of the residues **A** and **D** as α- and β-glucopyranoses, respectively, and **B** as the unit of the α-glucopyranuronic acid. Less easy was the identification of the mannopyranose residue **C** signals as the H-1/H-2 cross-correlation peaks were absent in the spectra, due to the small value of $^3J_{H\text{-}1,H\text{-}2}$ coupling constant. Much more useful to this regard was the NOESY spectrum (Fig. 2), that showed an NOE correlation between

Table 1. ^{1}H and ^{13}C NMR chemical shift (ppm) of K2 polysaccharide at 313 K and pD = 7

Residue	H-1/C-1	H-2/C-2	H-3/C-3	H-4/C-4	H-5/C-5	H-6/C-6
4-α-D-Glc*p* **A**	5.283	3.578	3.873	3.680	4.050	3.780; 3.780
	102.8	72.4	72.8	79.8	71.5	60.8
t-α-D-GlcA*p* **B**	5.152	3.528	3.775	3.490	4.084	—
	102.7	73.0	74.7	73.0	74.1	176.7
3,4-β-D-Man*p* **C**	4.769	4.212	3.839	4.042	3.580	4.029; 3.839
	101.0	71.9	82.1	73.3	76.5	61.0
3-β-D-Glc*p* **D**	4.518	3.370	3.630	3.530	3.530	3.725; 3.963
	103.5	73.3	83.5	71.5	77.4	62.0

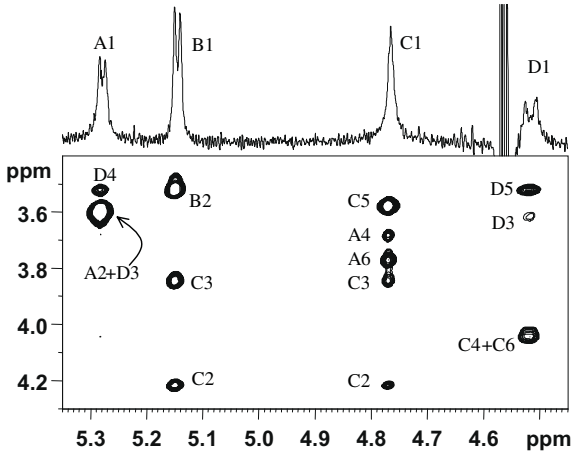

Figure 2. Expansion of the NOESY spectrum of *K. pneumoniae* K2 polysaccharide in D_2O at 313 K and pD = 7. The numbers indicate the protons involved in the NOE connectivities of each residue.

the anomeric proton of **C** unit and the signal at 4.212 ppm, which, on the basis of its low-field chemical shift, was assigned to the proton H-2 of the same unit. This last was COSY-correlated to the signal at 3.839 ppm, which was therefore identified as proton H-3 of unit **C**. The NOE contact between this proton and the proton at 3.580 ppm identified this last as H-5, according with the β-configuration of the residue **C**. The HSQC-DEPT experiment allowed the assignment of the ^{13}C resonances of both the methine and the anti-phase hydroxymethylene signals. The comparison of the carbon chemical shifts with those of the unsubstituted hexopyranoses confirmed the pyranose forms and the anomeric configurations of all of the four residues. In addition several low-field shifted ^{13}C signals supported the terminal location of the D-GlcA (**B**) residue and the substitutions at C-3 for D-Glc*p* (**D**), at C-4 for D-Glc*p* (**A**) and C-3 and C-4 for D-Man*p* (**C**), in agreement with the data of methylation analysis.

In order to define the sequence of residues and give insight into the secondary structure of the repeating unit an in-depth interpretation of experimental inter-residue NOE contacts (Table 2) was performed by molecular mechanic and dynamic calculations.

In the preliminary part of the analysis the optimal dihedral angles were evaluated for each glycosidic linkage constituting the repeating unit (Table 3), and when multiple minima were present, the lowest in energy was selected. These dihedral angles were used for the construction of the following decasaccharide unit:

B **B** B
↓ ↓ ↓
3 **3** 3

C→4A→**3D**→**4C**→**4A**→3**D**→4C

Table 2. Comparison of simulated proton distances (Å) versus experimental NOE data, only inter-residue contacts are considered

Proton contacts	Experimental NOE intensities	Averaged calculated distances
A1/**D**2	+	3.89
A1/**D**3	+++	2.34
A1/**D**4	++	3.48
A5/**D**3	++	3.25
B1/**C**2	+++	2.50
B1/**C**3	+++	2.32
B3/**D**2	++	3.08
B3/**D**4	++	3.33
B3/**D**6	++	3.12
C1/**A**4	+++	2.36
C1/**A**6+6′	+++	2.66 and 3.31
C2/**B**5	+++	2.86
C2/**A**4	+	4.06
C2/**A**6	++	3.25
C3/**B**5	++	3.42
D1[a]/**C**4	++	2.68
D1/**C**5	++	3.69
D1[a]/**C**6[b]	+++	2.25
D2/**A**5	++	2.77

Part of the experimental NOEs is shown in Figure 2.

[a] Overlapped cross-peaks. Intensities attribution is uncertain and based on simulation data.

[b] Only the proton **C**6 at 4.03 ppm is involved, in agreement with modelling data where only one of the two diastereotopic **C**6 proton is proximal to anomeric proton of **D** residue.

Table 3. Optimal dihedral angles and energy values (kJ/mol) estimated for each glycosidic junction calculated with MM3* force field and with $\varepsilon = 80$

Glycosidic junction	Oligosaccharide unit	Φ	Ψ	E
A→**D**	α-D-Glc-(1→3)-β-D-Glc	−61.3	−43.3	119.5
B→**C**	α-D-GlcA-(1→3)-β-D-Man	−35.2	+47.7	102.9
D→**C**	β-D-Glc-(1→4)-β-D-Man	+58.4	−6.4	118.2
C→**A**	β-D-Man-(1→4)-α-D-Glc	+60.8	−4.3	112.4

All the sugar residues in bold are those for which the simulated NOEs and averaged distances are calculated and reported in Table 2. This starting structure was minimized and successively submitted to molecular dynamic analysis approximating the water solvent with the GB-SA model. The oligosaccharide was kept in a thermal bath at 313 K and its dynamic behaviour was observed over 8 ns of simulation. Ensemble-average inter-proton distances for each molecule were extracted from dynamic simulations and translated into NOE contacts according to a full matrix relaxation approach; the averaged distances were compared with the experimental NOEs and showed a reasonable agreement. This analysis allowed the complete comprehension of all NOEs. During this analysis it was possible to confirm the presence of trivial NOEs, such as those connecting either inter-glycosidic or intra-residue protons, but also to identify some other dipolar effects whose interpretations could have been problematic. For instance, proton **C**1

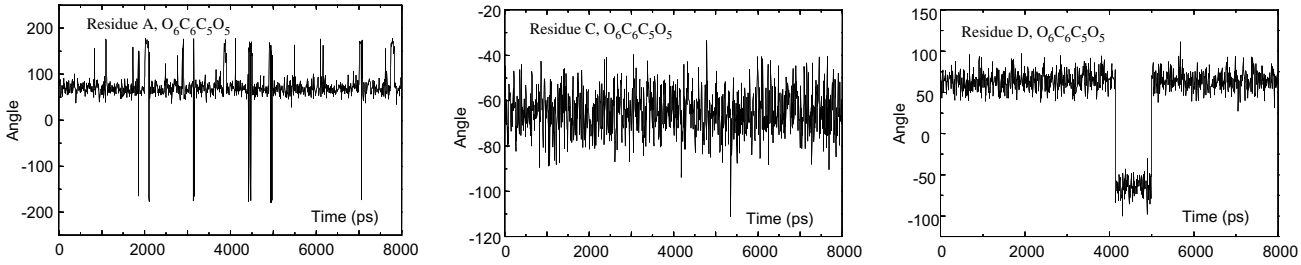

Figure 3. Monitoring of the exocyclic hydroxyl group orientations of residues **A** (left), **C** (centre) and **D** (right) during the molecular dynamic simulation.

showed a NOE cross-peak at about 3.77 ppm, an area of the spectrum where at least two different protons appeared: **B**3 and **A**6. On the basis of NOEs simulation, it was clear that only proton H-6 of **A** was involved in the NOESY correlation. Similar considerations were applied for proton **D**1 that showed a cross-peak correlation with proton **C**4 of unexpected good intensity. Simulation data analysis revealed that this NOE density was due to the contribute of two different cross-peaks: **D**1/**C**4 and **D**1/**C**6.

The deep involvement of the hydroxymethyl groups in the NOEs' correlation led to deepen the analysis of their conformation behaviour. The exocyclic hydroxyl orientations were considered at the stage of monosaccharide optimization. The oxygen atoms of primary alcohol groups were orientated according to the two possible conformations: *gt* and *gg* in order to avoid 1–5 interactions with the other oxygen atoms. The best orientation for each the exocyclic hydroxyl group was determined to be *gt*, *gg* and *gt* for residues **A**, **C** and **D**, respectively; these orientations were used for the construction of the larger molecule. The behaviour of these OH groups was checked throughout the simulation (Fig. 3). Residue **A** shows a preferential *gt* orientation, with almost no trace of the other possible one (*gg*): actually the hydroxyl group passes at $-60°$ only transiently. It is noteworthy that another conformation, not considered in the initial minimization steps, was described with the exocyclic hydroxyl group angle with a value of about 180°. This orientation is recurrent during the simulation suggesting that the total time was not too short but long enough to sample all of the conformational possibilities of the molecule. Similar considerations could be applied for residue **D**, where the inter-conversion between the two forms is clearly evidenced, with the second one less populated. This residue does not bear any substituent at carbon 4, making possible the occurrence of the *gg* conformer. Differently from the other two, residue **C** displays a preferential *gg* orientation of its O6, in agreement with the experimental data, where only one of the two diastereotopic H6 is dipolar coupled with proton **D**1, indicating a rather rigid orientation of the O6C6C5O5 torsion angle in the *gg* conformation.

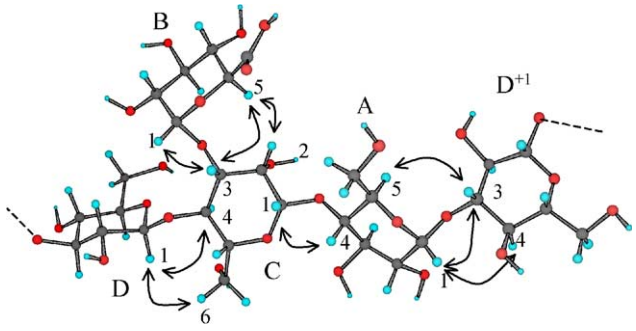

Figure 4. 3D model of the repeating unit of the K2 polysaccharide from *K. pneumoniae* strain 52145. More relevant NOEs are indicated by arrows. Glucose unit $\mathbf{D}^{+1}$, belonging to another repeating unit, has been included in the picture in order to evidence all the experimental NOEs.

In conclusion in this letter we reported a complete assignment of ^{1}H and ^{13}C NMR chemical shifts of the K2 *K. pneumoniae* polysaccharide repeating unit together with a proposed model of its secondary structure (Fig. 4).

1. Experimental

1.1. CPS isolation

K. pneumoniae wabH waaL double mutant strain was routinely maintained in and grown in LB agar medium.[7] Cultures for analysis of CPS were grown in Trypticase Soy Broth (TSB) at 37 °C. CPS was isolated from cells by phenol–water extraction.[8] The water phase fraction (150 mg) was chromatographed on a Butyl Sepharose column (Pharmacia). The column (40×2.5 cm) was equilibrated with 200 mM NaOAc pH 4.7 and initially eluted with 150 mL of the same buffer and then with 450 mL of a linear gradient NaOAc/*n*-PrOH (50:50 v/v). Fractions (2.5 mL) were collected and monitored for carbohydrates (phenol/sulfuric acid test: A at 490 nm). On the basis of the chromatographic profile the eluted fractions were pooled, dialyzed and freeze dried. Fractions **1**, **2** and **3** of 16, 29 and 34 mg, respectively, were obtained. Fraction **1**, which contained

mainly CPS was hydrolyzed with 1% AcOH containing 0.1% of SDS at 100 °C for 3 h. After cooling the sample was centrifuged (10,000*g*) for 20 min. The supernatant was lyophilized, washed with ethanol and purified on a Sephacryl S-300 column (Pharmacia), giving the capsular polysaccharide (4 mg).

1.2. Chemical analyses

The glycosyl analysis was performed on a sample of CPS (1 mg) dried over P_2O_5 overnight. This sample was treated with 1 M HCl/CH_3OH (1 mL) at 80 °C for 20 h, neutralized with Ag_2CO_3, dried and acetylated. The acetylated sample was subjected to the GLC–MS analysis.

The methylation analysis was performed on a CPS sample (1 mg) previously deionized by adding Dowex 50WX resin (H^+ form) and then dried on P_2O_5 for 20 h. The sample was dissolved in anhydrous DMSO and methylated as reported.[9] Linkage analysis was performed as follows: the methylated sample was carboxymethyl reduced with lithium triethylborodeuteride (Aldrich), then totally hydrolyzed with 2 M trifluoroacetic acid at 120 °C for 120 min, reduced with $NaBD_4$ and finally acetylated as described.[10]

The absolute configuration analysis was carried out by treating a sample of CPS (1 mg) with 1 M HCl/MeOH (500 μL) overnight at 80 °C. After neutralization and drying, the crude reaction was dissolved in CH_3OH, converted into octyl glycosides as described[6] and analyzed by GLC–MS.

All the samples were analyzed on a Agilent Technologies 5973N MS instrument equipped with a 6850A Gas Chromatography and an RTX-5 capillary column (Restek, 30 m × 0.25 mm i.d., flow rate 1 mL min^{-1}, He as carrier gas). Acetylated methyl glycosides analysis was performed with the following temperature program: 150 °C for 5 min, 150→250 °C at 3 °C min^{-1}, 250 °C for 10 min. For partially methylated alditol acetates the temperature program was: 90 °C for 1 min, 90→140 °C at 25 °C min^{-1}, 140→200 °C at 5 °C min^{-1}, 200→280 °C at 10 °C min^{-1}, 280 °C for 10 min. Analysis of acetylated octyl glycosides was performed as follows: 150 °C for 5 min, 150→240 °C at 6 °C min^{-1}, 240 °C for 5 min.

1.3. NMR spectroscopy

The ^1H and ^{13}C NMR spectra were recorded in D_2O at 400 and 100.0 MHz, respectively, with a Bruker DRX 400 Avance spectrometer equipped with a reverse probe, in the FT mode at 313 K. ^1H and ^{13}C chemical shifts are expressed in δ relative to acetone (2.222 and 30.2 ppm, respectively). The intensity ratio of proton signals was estimated by an ^1H NMR spectrum performed with an inter-pulsed delay of 3 s. Two-dimensional homonuclear and heteronuclear NMR spectra (COSY, HMBC, HSQC, HSQC-DEPT, NOESY, TOCSY) were recorded using standard Bruker software, mixing time of 100 ms was used for TOCSY spectrum.

Different NOEs spectra were acquired, with different mixing time (100, 150 and 200 ms) and at different temperatures. These spectra displayed similar cross-peaks, whose intensities were attenuated at short mixing times. NOESY spectrum recorded at 313 K with 200 ms showed the best cross-peak intensities without artefacts due to spin diffusion. This spectrum was then selected as a reference for the simulation data.

1.4. Molecular mechanics and dynamics calculation

Molecular mechanic and dynamics calculations were performed using the MM3* force field as implemented in MacroModel 8.0, installed under Red Hat 8 operative system. The MM3* force field used[11] differs from the regular MM3 force field in the treatment of the electrostatic term, since it uses charge–charge instead of dipole–dipole interactions. Molecular mechanic approach has been used to evaluate the optimal dihedral angles (Table 2) for each glycosidic junction, the calculations were performed for a dielectric constant $\varepsilon = 80$, as an approximation for the bulk water. Relaxed energy maps were calculated employing the DRIV utility (modulated with the DEBG option 150, which imposes to the program to start each incremental minimization reading the initial input structure file), more in detail, for each disaccharide entity, both Φ and Ψ were varied incrementally using a grid step of 18°, each (Φ, Ψ) point of the map was optimized using 2000 P.R. conjugate gradients, Φ is defined as H_1–C_1–O–$C_{aglycon}$ and Ψ as C_1–O–$C_{aglycon}$–$H_{aglycon}$.

On the basis of the values obtained, the selected oligosaccharide was built employing the optimal dihedral angles found (when two minima were present, the lowest in energy was considered), and minimized again with MM3* force field, but approximating water solvent using the GB/SA model. Molecular dynamic simulation started from this optimized structure, subjected to an equilibration time of 200 ps, and successively kept in a thermal bath at 313 K for 8000 ps, a dynamic time step of 1.5 fs together with the SHAKE protocol to the hydrogen bonds was applied, coordinates were saved every 4 ps of simulation leading to the collection of 2000 structures.

Ensemble-average distances between intra- and inter-residue proton pairs were obtained from the calculations and employed for the simulation of the experimental NOESY spectra, using a full matrix relaxation approach according to the program NOEPROM.[12] In particular, the spectra were simulated from the average distances $\langle r^{-6}\rangle kl$ calculated from the dynamic simulation at 313 K, assuming an isotropic motion of the molecule. A τ_c of 7000 ps was used to obtain the best match between experimental and calculated NOEs for the intra-residue proton pairs. In this case, integration of

two NOEs cross-peak density was performed in order to compare the experimental volume with the simulated one, the cross-peaks selected were the intra-residue correlations **B**1/**B**2 and **C**1/**C**2. The simulated NOEs were then compared to the experimental ones, these last were evaluated directly on the 2D spectrum counting the number of the contours in the 2D plot, and unfortunately rigorous volume integration was not feasible due to the overlapping of some of the interested densities. Exocyclic orientations of residues **A**, **C** and **D**, described from the dihedral angle O6–C6–C5–O5, was extracted from the simulation data using SuperMap, a program provided with the NOEPROM package and their time-dependence (Fig. 3) was visualized with the graphical program ORIGIN.[13]

Acknowledgements

This work was supported by grants of Ministero dell'Università e della Ricerca Scientifica (Progetti di Rilevante Interesse Nazionale 2004—U.O.M.P.). J.T. and M.R. were supported by Plan Nacional de I + D (Ministerio de Ciencia y Cultura, Spain).

References

1. Podschun, R.; Ulmann, U. *Clin. Microbiol. Rev.* **1998**, *11*, 589–603.
2. Gahan, L. C.; Sandford, P. A.; Conrad, H. E. *Biochemistry* **1967**, *6*, 2755–2766.
3. Sutherland, I. W. *J. Gen. Microbiol.* **1971**, *70*, 331–338.
4. Nassif, X.; Fournier, J. M.; Arondel, J.; Sansonetti, P. J. *Infect. Immun.* **1989**, *57*, 546–552.
5. Izquierdo, L.; Fresno, S.; Merino, S.; Corsaro, M. M.; De Castro, C.; Parrilli, M.; Naldi, T.; Regué, M.; Tomás, J. M., submitted for publication.
6. Leontein, K.; Lindberg, B.; Lönngren, J. *Carbohydr. Res.* **1978**, *62*, 359–362.
7. Miller, J. H. *Experiments in Molecular Genetics*; Cold Spring Harbor Laboratory Press, Cold Spring Harbor: New York, 1972.
8. Westphal, O.; Jann, K. *Methods Carbohydr. Chem.* **1965**, *5*, 83–91.
9. Hakomori, S. *J. Biochem. (Tokyo)* **1964**, *55*, 205–208.
10. Corsaro, M. M.; Evidente, A.; Lanzetta, R.; Lavermicocca, P.; Molinaro, A. *Carbohydr. Res.* **2001**, *330*, 271–277.
11. Allinger, N. L.; Yuh, Y. H.; Lii, J. H. *J. Am. Chem. Soc.* **1989**, *111*, 8551–8566.
12. Asensio, J. L.; Jiménez-Barbero, J. *Biopolymers* **1995**, *35*, 55–75.
13. ORIGIN, more information are available at: http://www.originlab.com/.